Functionalization of pectin-depleted residue from different citrus by-products by high pressure homogenization

Novita I Putri*, Miete Celus, Jelle Van Audenhove, Raymond P Nanseera, Ann Van Loey, Marc Hendrickx**

Laboratory of Food Technology and Leuven Food Science and Nutrition Research Centre (LFoRCe), Department of Microbial and Molecular Systems (M2S), KU Leuven, Kasteelpark Arenberg 20, Box 2457, 3001, Leuven, Belgium

*corresponding author during submission :
novitaika.putri@kuleuven.be
+32 16 37 64 73

**corresponding author post-publication :
marceg.hendrickx@kuleuven.be
+32 16 32 15 72

Declarations of interest : none

ABSTRACT

In the valorisation of fruit and vegetable by-products by high pressure homogenization (HPH) into texturizing ingredients, the source of the by-product is an important determining factor. This study aims to demonstrate the valorisation potential of citrus residues after acidic pectin extraction (AR)

and to investigate differences between citrus species (lemon, orange, grapefruit) and fruit parts (peel and pulp) as the source of the residues. Based on the results, pectin extraction is favourable in improving the storage modulus (G') of the residue. However, residual pectin content in the different ARs, as indicated by pectic monosaccharides (e.g., GalA, Rha, Fuc), did not correlate to G' after HPH. The G' of all ARs suspensions, regardless of the source, improved significantly after HPH at 20 MPa. After HPH, fragmentation and subsequently aggregation of particles were observed from the particle size reduction and microscopy visualization. Particle morphology and size did not correlate with the G' of the suspensions. Residual pectin's Rhamnogalacturonan-I contribution and degree of methyl-esterification, protein content, and glucose content related to hemicellulose were correlated to the G' of the suspensions before HPH. However, after HPH, no correlation was found between G' and these characteristics, likely due to changes on the structure of the particles. The results highlight the high potential of all the citrus ARs from the different sources to be functionalized as texturizing ingredients. However, the peel AR from grapefruit and lemon exhibited better rheological properties and may be considered as better sources compared to the other citrus by-products.

Keywords : citrus by-products, cell wall material, high pressure homogenization, rheology

1. Introduction

Citrus fruits are one of the massively cultivated crops in the world. Around 144 million tons of citrus were produced worldwide in 2019. About 40-50% of the harvested fruits go into the processing industries (FAO, 2021). From the processed fruits, 50-60% becomes waste with very high organic matter content (Satari & Karimi, 2018). Thus, a significant amount of by-product is created which may be costly for the company to discharge and be a burden to the environment.

As the concept of circular economy is becoming more relevant, it will be in the interest of the industry to use these by-products as a resource for further production, thus ensuring less waste. Consequently, research in the valorisation of by-products from the food processing industry and in particular the citrus processing industry, becomes more essential.

Many efforts in the valorisation of citrus by-products have been made, for example as animal feed, as compost or as a source in the biorefinery process to produce biofuel, biogas and ethanol (Zema et al., 2018). Research has been carried out to incorporate fibres from the citrus by-products into food productions either to improve the product's nutrition and/or physical properties, for example in bakery products (Caggia et al., 2020; Korus et al., 2020), meat products (Fernandez-Gines et al., 2003; Song et al., 2016) and dairy products (Sendra et al., 2010). The incorporation of citrus fibre led to quality improvement in some products, but in the other hand, it may also cause detrimental effects such as harder texture in sausage or lower bread volume (Fernandez-Gines et al., 2003; Korus et al., 2020).

In food industry, pectin extraction from citrus by-products has been widely done to manufacture different citrus based pectins. However, pectin extraction still leaves a substantial amount of residue since pectin only comprises a portion of the by-product. The residue left mostly contains cell wall materials (CWM) such as cellulose, hemicellulose, residual pectin and protein which could still have various functional properties, for example a thickening capacity. This CWM in the residue can be developed into a natural ingredient that can be used in food production. Previous study has shown that the CWM in the residue can be functionalized into a texturizing ingredient with good rheological properties using high pressure homogenization (HPH) (Willemsen et al., 2018).

The ability of HPH to improve the rheological properties of various fruit and vegetable dispersed systems has been shown by several studies (Atencio et al., 2021; Augusto et al., 2012; Bengtsson & Tornberg, 2011; Huang et al., 2020; Su et al., 2020; Van Audenhove, et al., 2021; Willemsen et al., 2017; Zhou et al., 2017). However, the response of fruit and vegetable CWM after HPH is not the same for all the matrices studied. On the one hand, some studies showed an improvement of the dispersion's rheological properties after HPH, for example with tomato, mango, citrus, pumpkin and sugar beet (Huang et al., 2020; Lopez-Sanchez et al., 2011; Su et al., 2020; Van Audenhove et al., 2021; Willemsen et al., 2017; Zhou et al., 2017). On the other hand, the rheological properties of carrot, broccoli, onion and apple based dispersions were not improved or even degraded after HPH (Bengtsson & Tornberg, 2011; Lopez-Sanchez et al., 2011; Van Audenhove et al., 2021). This discrepancy highlights the importance of the CWM source and its characteristics during the functionalization of the fruit and vegetable by-products using HPH.

This study is divided into two parts, the first part aims to demonstrate the potential of the residue obtained after acid pectin extraction (further referred to as acid residue), with extraction conditions similar to those performed in food industry, to be functionalized into a texturizing ingredient and to discuss the role of the pectin extraction on the functionalization of the CWM. The second part focuses on the effect of the CWM source on the functionalization, in which by-products from three different citrus species, i.e., lemon, orange and grapefruit, and two different parts of the fruit, i.e., the peel and the pulp, were studied. Different acid residues from the various citrus materials may lead to varying CWM characteristics and consequently they may have different responses to the functionalization process using HPH. In the second part, the difference in the CWM characteristics obtained from different citrus by products, the rheological properties of the CWM suspensions and the correlation between them will be discussed in order to give insight into the functionalization potential of the by-products as a texturizing ingredient.

2. Materials and methods

2.1. Materials

In the first part of the study, industrial citrus by-products, specifically frozen lemon peel (I-L-PE) and pulp (I-L-PU) obtained from Cargill (Vilvoorde, Belgium) were used. Prior to further processing, the peel and pulp were thawed and then ground using a food processor (Braun MR 5550 M CA, Kronberg, Germany). In the second part, fresh lemon (L), orange (O) and grapefruit (G) were obtained from the local market and then peeled using an automatic peeler (Pelamatic Orange Peeler Pro, Valencia, Spain). The flavedo (outer skin) was separated during the first peeling and the albedo was collected as the peel residue sample (PE) after the second peeling. The peel was then ground using the same food processor as above to reduce the size before further processing. The peeled fruits were juiced using an Angel Juicer 8500 S (Naarden, Netherlands) and the pulps were collected as the pulp residue sample (PU).

Eight monosaccharides were used as a standard solution in sugar content analysis. D-(+)-galacturonic acid monohydrate and L-(-)-fucose were obtained from Sigma Aldrich (Diegem, Belgium). L-(+)-rhamnose monohydrate was from Acros Organic (Geel, Belgium). L-(+)-arabinose was from Fluka Biochemika (Buchs, Switzerland), D-galactose was from Merck (Darmstadt, Germany), D-(+)-glucose monohydrate was from Riedel-de-Haën (Seelze, Germany), D-(+)-xylose was from UCB (Leuven, Belgium) and D-(+)-mannose was from Fluka Analytical (Buchs, Switzerland). Other chemicals used in this study were all analytical grade unless stated otherwise.

2.2. Alcohol insoluble residue separation

Alcohol insoluble residue (AIR) separation were carried out on all raw materials in order to isolate the cell wall materials from the by-products. AIR was obtained using the method described in McFeeters & Armstrong (1984). Approximately 30 grams of the fresh citrus peel or pulp was suspended in 192 ml technical ethanol 99% (v/v), blended (Buchi mixer B-400, Flawil, Switzerland) and then vacuum filtered (Machery-Nagel MN 615 Ø 90 mm). The process of resuspension and filtration were repeated two times on the residue after filtration with 96 ml technical ethanol 99% (v/v) and then 96 ml technical acetone. The residue after the final filtration was collected as AIR and dried in an oven overnight at 40 °C.

2.3. Pectin acid extraction

Pectin acid extraction on AIR was performed in duplicate for each residue type following the procedure reported by Willemsen et al. (2017). Sixty grams of AIR were suspended into 4 L of demineralized water at 80 °C for 30 minutes. Nitric acid (7N) was added to the suspension drop by drop until the pH reached 1.6 and the extraction was continued at 80 °C for 1 hour with constant mixing at 300 RPM. After cooling to room temperature in an ice bath, the suspension was centrifuged at 4000 g for 10 minutes at 20 °C to separate the pectin-rich supernatant and the pectin-depleted acid residue (AR). The AR was washed with demineralized water and then filtered using filter paper (Machery-Nagel MN 615 Ø 125 mm). The AR was frozen until further analysis or processing.

2.4. High pressure homogenization of the citrus residues

The citrus AIR and AR were functionalized using HPH following the method described in Willemsen et al. (2017). The AIR and AR were resuspended with standardized tap water (0.2% NaCl and 0.015% $CaCl_2.H_2O$ in ultrapure water) at 2% w/w solid concentration. The pH of the suspension was adjusted to 4.5 using 2M Na_2CO_3 and was left overnight with constant stirring. The pH value of 4.5 were chosen based on a previous study (Willemsen et al., 2018) that showed pH 4.5 as the optimum value for the cell wall functionalisation with HPH for citrus CWM. Prior to the HPH, the suspension was pre-mixed using Ultra-Turrax with S 25 N – 25 G Dispersing Tool (IKA, Satufen, Germany) at 8000 RPM for 10 minutes. The non-homogenized sample (0 MPa) was collected at this point. The suspension was then homogenized at 20 MPa using a Panda 2k NS 1001L (GEA Niro Soavi, Parma, Italy).

2.5. Rheology analysis of the suspension

Rheology analysis was done in duplicate for each citrus residue suspension according to the method described in Willemsen et al. (2018). Rheological measurements of the fibre suspension before and after HPH were performed using an Anton Paar MCR302 rheometer (Graz, Austria) at 25 °C. A custom built cup and concentric cylinder with conical bottom were used. The surface of the geometry and the cup were sandblasted with average surface roughness between 50 and 100 µm to prevent wall slip effects. The gap between the cylinder and the cup was 2 mm. Pre-shear of the sample (at 10 s^{-1} for 30 s, followed by 30 s rest) was done to avoid loading history. A strain sweep (0.01 % to 100% strain) was performed on each of the suspensions at a fixed frequency of 6.28 rad/s. A frequency sweep measurement was also carried out in the angular frequency ranged from 628 to 0.628 rad/s at a constant strain of 0.1% (within the LVR as confirmed by strain sweep test) to obtain the storage and loss moduli.

175 *2.6. Microscopy analysis of particles in the suspension*

176

177 The microstructure of non-homogenized and homogenized suspensions was visualized by
178 microscopy. Each suspension was diluted to obtain a solid concentration of 0.6% (w/w) to
179 visualize the cell wall material (Van Audenhove, et al., 2021). Light microscopy was performed on
180 the diluted suspension using an Olympus BX-41 microscope (Olympus, Optical Co. Ltd, Tokyo,
181 Japan), equipped with an Olympus XC-50 digital camera and photo-analysing software in
182 differential interference contrast mode (Willemsen et al., 2017).

183

184 *2.7. Particle size distribution analysis of the suspension*

185

186 The particle size distribution of each suspension before and after HPH was analysed using laser
187 diffraction (Beckman Coulter, LS 13 320, Miami, Florida). The detection range was 0.04 to 2000
188 µm, achieved using laser light with a wavelength of 750 nm as the main light source and laser
189 light with wavelength 450, 600 and 900 nm as polarization intensity differential scattering. The
190 volumetric particle size distribution was calculated from the intensity of the scattered light
191 according to the Fraunhofer optical model (plant cell wall RI = 1.6, water RI = 1.33 and dispersion
192 absorption coefficient = 1) (Verrijssen et al., 2014). Two runs of analysis were carried out for each
193 loaded samples and for each suspension, two times loading were done.

194

195 *2.8. Characterization of the citrus acid residue*

196 Prior to all chemical analyses, the citrus AR was dialyzed to remove the ions that may interfere
197 with the analyses. Therefore, the AR samples were suspended in demineralized water and the
198 pH was adjusted to 6 with 0.1 M NaOH. The samples were transferred into Spectra/Por® dialysis

tubing (3.5 kDa, MWCO) and were dialyzed against demineralized water for 48 h. The dialyzed sample was then freeze-dried to obtain dry samples for analysis.

2.8.1. Galacturonic acid content analysis

Hydrolysis of the sample prior to galacturonic acid (GalA) analysis was done using the method described by Ahmed & Labavitch (1977). Freeze dried AR (10 mg) was hydrolysed by adding 8 ml concentrated H_2SO_4 (98%) into the sample in an ice bath. The solution was then stirred and subsequently, 4 ml demineralized water were added to the solution dropwise. After 1 hour of hydrolysis with constant stirring, the solution was diluted to 50 ml with demineralized water. The uronic acid assay was carried out according to the method in Blumenkrantz & Asboe-Hansen (1973). The GalA content was determined by adding 3.6 ml 0.0125 M sodium tetraborate in 98% H_2SO_4 into 0.6 ml of the diluted hydrolysates and then heated for 5 minutes at 100 °C. After cooling to room temperature, the solution was mixed with 60 µl of m-hydroxydiphenyl-solution (0.15% metahydroxydiphenyl in 0.5% NaOH) for 1 minute and the intensity of the colour formed after another 1 minute was measured as absorbance at 520 nm using a spectrophotometer (Spectrophotometer Genesys 30 Vis, Thermo Fisher, Waltham, MA, USA). A blank was included for each sample using 60 µl of 0.5% NaOH instead of m-hydroxydiphenyl-solution. GalA content was calculated using a standard calibration curve. Hydrolysis for GalA analysis were done in duplicate and the spectrophotometry analysis were done in triplicate for each hydrolysed sample.

2.8.2. Residual pectin's degree of methyl-esterification

The degree of methyl-esterification (DM) of residual pectin present in each citrus AR sample was determined in triplicate using Fourier Transform Infra-Red (FT-IR) Spectroscopy according to the

method described in Kyomugasho et al (2015). The freeze-dried sample was compressed to create a compact sample without air bubbles and smooth surface. The transmittance of the sample was measured at wave numbers 4000 cm^{-1} to 400 cm^{-1} at a resolution of 4 cm^{-1} using Shimadzu FTIR-8400S (Japan). The mean spectrum was obtained after 100 runs and was converted into absorbance. Peak deconvolution was performed to minimize the protein interference, which resulted in spectra with individual peaks centred at approximately 1650 cm^{-1} and 1540 cm^{-1} for protein and at approximately 1740 cm^{-1} and 1600 cm^{-1} corresponding to the ester carbonyl group (C=O) in the methylated carboxyl groups and carboxylate group (COO^-) in the non-methylated carboxyl groups, respectively. The DM of the pectin was determined using the calibration curve equation developed by (Kyomugasho et al., 2015) with the deconvoluted spectra:

$$Y = 123.45X + 6.5914$$

where Y is the DM (%) of the pectin in the sample and X is the ratio of absorbance intensity of the 1740 band over total intensity of the 1740 and 1600 band.

2.8.3. Neutral sugar content analysis of the citrus acid residues

Neutral sugar content of each AR sample was determined using the method described by Yeats et al. (2016) with some modifications. The neutral sugars analysed were Fucose (Fuc), Rhamnose (Rha), Arabinose (Ara), Galactose (Gal), Glucose (Glu), Xylose (Xyl), and Mannose (Man). Freeze dried samples (2 mg) were mixed with 100 µl of 72% (w/w) H_2SO_4 for 1 hour. Afterwards, 2.8 ml ultra-pure water was added to dilute the sulfuric acid to 4% (w/v) and the sample was hydrolysed by heating the solution at 121 °C for 1 hour (Saeman hydrolysis). Another set of samples were directly mixed with 4% (w/v) sulfuric acid and hydrolysed (matrix hydrolysis). Saeman hydrolysis was done to completely hydrolyse all cell wall polysaccharides including

cellulose, while the matrix hydrolysis was done to hydrolyse the non-cellulosic cell wall polysaccharides. After hydrolysis, the solution was neutralized using 2.32 ml of 1 M NaOH and then diluted to 10 ml. The diluted solutions with visible unhydrolyzed solid particles were centrifuged at 4°C for 10 minutes at 20000 g. The solution was then frozen until further analysis.

Analysis of the neutral sugars was done using High Performance Anion Exchange Chromatography with Pulsed Amperometric Detection system (Dionex ICS-6000). The hydrolysed solution was further diluted if necessary to fit the calibration curves and then filtered with 0.20 µm Chromafiol (Macherey-Nagel, Düren, Germany). A volume of 10 µl of the diluted sample solution was injected and separated on a CarboPac PA-20 column equipped with guard column to obtain a chromatogram of the sugars. The sample was eluted with 2 mM NaOH (to obtain the value of Fuc, Gal, Glu, Xyl, and Man) and 18 mM NaOH (to obtain the value of Rha and Ara). The hydrolysis and injection were done twice for each AR. The concentration of the sugars was determined by injecting standard solutions at various concentrations (0.5-12 ppm) to create calibration curves. The concentrations obtained were corrected with factors from hydrolysed standard sugar solution.

2.8.4. Protein content analysis of the citrus acid residues

The protein content in the citrus AR was determined by the Dumas combustion method (AOAC, 2006). The nitrogen content of the samples was determined and then converted into protein content using a conversion factor of 6.25. The analysis was done three times for each AR.

2.9. Statistical analysis

The statistical differences (α = 0.05) between means were analysed using Two-Way ANOVA. Pairwise comparison was done with Tukey-HSD test to compare means between the different citrus species if significant interactions ($p \leq 0.05$) were detected. Correlation study between the citrus AR characteristics and the rheological properties were done using Pearson Correlation. All statistical analysis were done using JMP Pro 15.1.0.

3. Results and Discussion

3.1. The role of pectin extraction and HPH on the functionalisation of lemon CWM

In order to demonstrate the potential of the citrus by-products after pectin extraction to be functionalized into texturizing ingredients, in the first part of this study, both AIR (before pectin extraction) and AR (after pectin extraction) samples from industrial lemon peel and lemon pulp by-products were functionalized with HPH. The rheological properties of suspensions made from the AIR and AR, both before and after HPH, were analysed and compared. The AR sample from the lemon peel contains 15.3% GalA, corresponding to 15.9% of the GalA originally present in the AIR, and the lemon pulp sample have 17.1% GalA , corresponding to 22.5% of the GalA originally present in the AIR (Table 1). GalA is here used as an indicator for pectin. The monosaccharides and protein content of these samples can be seen in Table S-1 of the Supplementary File.

In order to determine the rheological properties of all the suspensions, strain sweep tests were carried out to identify the Linear Viscoelastic Region (LVR). The storage modulus (G') of all the citrus CWM suspension remains constant (in LVR) at 0.1% strain; thus, this strain value was used when carrying out the frequency sweep. To compare the rheological properties of AIR and AR

suspensions, one point in the frequency sweep (at ω 6.28 rad/s) was selected (Figure 1). Suspensions from the AIR of lemon peel and pulp have substantially lower G' compared to suspensions from AR. After HPH, the AIR suspensions also did not show significant improvement in the G' meanwhile the AR suspensions showed the potential to be functionalized into suspensions with considerably higher G'. Thus, the acidic pectin extraction process that was performed on the AIR of lemon peel and pulp is favourable in the functionalization of citrus by-products. This also highlights the potential to valorise the residue or waste from the pectin manufacturing into a texturizing ingredient.

Pectin extraction is beneficial to the functionalisation of the residual CWM since it can disentangle and open up the cell wall network. These results are in line with previous studies hypothesizing that pectin extraction is advantageous in the functionalization of the citrus cell wall materials, especially the lemon peel and pulp. The rheological properties of citrus fibre suspension without prior pectin extraction in a previous study (Su et al., 2019) was poorer than in the present study, even though the same solid concentration and even higher pressure of HPH were used. Willemsen et al. (2017) also showed that when pectin were increasingly extracted from lemon peel, the residue can be functionalized into suspensions with higher storage modulus.

The improvement in the rheological properties of AR suspensions after HPH happened due to several mechanisms that have been hypothesized. First is the opening of the cell wall network after HPH. It has been reported that cellulose particles had a higher porosity after 2-16 passes of HPH at 15 MPa (Ulbrich & Flöter, 2014). The particles are also broken down due to the shearing during HPH, causing changes in the microstructure, and this leads to the exposure of more hydrophilic groups (Su et al., 2019). Cell fragmentation can also expose other cell wall constituents such as pectin and protein. These changes can improve interparticle interactions and

eventually aggregation of particles that can promote water imbibition and formation of the weak gel network (Augusto et al., 2012). Secondly, the solubilization of some initially insoluble polysaccharides after HPH could increase the viscosity of the continuous phase of the suspension (Huang et al., 2020; Van Audenhove et al., 2021; Zhou et al., 2017). Bengtsson & Tornberg (2011) also observed that in tomato CWM with less insoluble pectin content, the microstructural changes such as cell fragmentation after HPH can be more drastic, while in carrot and potato with higher insoluble pectin content, the CWM are more resistant to the microstructural change due to HPH.

3.2. Functionalisation of citrus ARs from different raw materials

3.2.1. Changes in the rheological properties of the different citrus ARs after HPH

ARs from three different citrus fruit (grapefruit, orange, lemon) and two different part (peel and pulp) were functionalized using HPH and the change in the rheological properties after HPH were measured. From the results of the strain sweep test (Figure 2), two notable observations will be discussed. First, comparing the G' in the low strain region, the decline of the G' from the LVR happened at different strain points between non-homogenized and homogenized suspension for all type of materials. The G' values of non-homogenized suspensions dropped to 90% of the constant value in the LVR at approximately 0.6% strain whereas the homogenized suspensions' G' dropped at strain > 1%. This indicates that after HPH, the suspensions have stronger structure in the low strain region. The same observation was reported on the CWM suspensions from other matrices (Van Audenhove et al., 2021)

Second, looking at the G' in the high strain region (Figure 2), two distinct large amplitude oscillatory shear (LAOS) behaviours as described in Hyun et al. (2002) were observed, i.e. Type

I behaviour (strain thinning) and Type III behaviour (weak strain overshoot). Hyun et al. (2002) suggested that the two distinct behaviours are related to the microstructure of the particles in the system. Type I behaviour relates to chains of polymers with certain entanglement in which as the strain increases, the chain orientation or alignment along the flow direction caused a decrease in the moduli. Type III behaviour, on the other hand, were observed in a disordered and extended polymer dispersion system with association (for example with hydrogen bonding) in the polymers, causing a formation of a complex structure. In the present study, Type III behaviour was clearly observed on suspension from grapefruit peel AR both before and after HPH and on orange and lemon peel AR suspension before HPH. Conversely, orange and lemon AR suspension after HPH and all the pulp AR suspensions did not show a weak strain overshoot and instead showed a Type I behaviour.

Previous studies (Huang et al., 2020; Su et al., 2020) reported a shift from Type I to Type III behaviours after the HPH of citrus fibre and sugar beet pulp suspension with the same solid concentration and similar range of HPH pressure as the citrus suspension in the present study. The researchers argued that the shift from Type I to Type III behaviour indicated that the structure of the network in the suspension has more particles interactions (entanglement) after HPH. Contrary to the previous studies, a shift from Type III to Type I behaviour after HPH was observed in the orange and lemon peel AR suspensions. Even in the grapefruit AR suspension, the maxima of the G" after HPH were also less prominent. However, the shift from Type III to Type I in this study did not directly translate to a weaker structure as implied by previous studies. The different observations between the previous and the present study may indicate that the CWM suspensions of the citrus AR show a different microstructure with different mechanisms of network formation. The difference in the microstructure may result from the pectin extraction step that was carried out in this study which may alter the interactions in the network of the CWM. A study has

374 shown that there are different interactions between particles in plant particle dispersions which
375 correlate to the microstructure of the particles. This study suggested that flocculated particles may
376 have interactions due to attractive forces, smooth particles may interact through repulsive forces
377 and particles with rough edges may interact through entanglement can forming network due to
378 the static friction. Different interactions (and concentrations of the particles) can affect the particle
379 packing which will lead to a different rheological behaviour (Lopez-Sanchez et al., 2012).
380
381 From the frequency sweep test, the G' and G" of the suspensions from different AR as a function
382 of frequency (ω) were obtained. All the suspensions both before and after homogenization show
383 higher G' values than the G" and the moduli were dependent on the ω with positive slope (Figure
384 S-1 in Supplementary File). This indicates that the suspensions exhibit an elastic behaviour rather
385 than plastic or viscous and have weak gel properties (Barnes, 2000; Rao, 2014). The G' of the
386 suspensions made from different citrus fruit ARs at a frequency of 6.28 rad/s are shown in Figure
387 3. An increase of 51-216% in the G' of the suspensions after HPH were observed. This
388 improvement in the rheological properties occurred in all the citrus AR suspensions regardless of
389 the citrus species or the citrus part.
390
391 In this study, although increases in the G' were detected on all the citrus AR suspensions after
392 HPH, the rheological properties of suspensions from the different citrus ARs were not similar.
393 After HPH, the peel AR suspensions had higher G' compared to the pulp for each of the citrus
394 species. Suspensions from orange AR after HPH had the lowest value of G' among the citrus
395 species meanwhile lemon and grapefruit AR suspensions had high G' without any significant
396 difference between them. The difference in the response after HPH among the different citrus AR
397 may have some correlations with the microstructure and other characteristics of the residue. The

correlations and the possible effect of the different citrus AR characteristics on the rheological properties of the suspension will be discussed below.

3.2.2. Effect of the physical and chemical properties of citrus AR on the rheological properties

3.2.2.1. Particle morphology

The microstructure for each of the citrus ARs was characterized by light microscopy visualization shown in Figure 4. Before HPH, the particles in the citrus residue had different morphology between the different type of residues. Citrus AR from the pulp had fibrous morphology while the peel AR had broken cell wall fragments which are irregularly shaped. The fibrous particles in the pulp AR, which were rod-like shaped, have a higher phase volume compared to other particle morphologies such as sphere or disc and therefore theoretically should cause the suspension with such particles to have higher G' (Barnes, 2000). This theory is true for the non-homogenized suspension of the citrus AR where the G' of the orange pulp and lemon pulp suspensions was higher than the peel counterparts, albeit not significant. Contrary, the G' of the non-homogenized grapefruit peel AR suspension were higher than the pulp counterpart, although also insignificantly. However, the particles in the grapefruit peel AR were quite elongated, almost similar to the rod-shaped fibrous particles in the pulp, which indicate a high phase volume leading to a higher G'.

Contrary to the observations before HPH, suspensions from the pulp samples after HPH have lower G' values compared to the peel suspensions. It is possible that the fibrous particles in the pulp suspensions were broken down by HPH in a way that did not encourage particle interactions which lead to less particle aggregation, meanwhile the irregularly-shaped peel particles were more easily aggregated to form a network leading to suspensions with higher G'. Previous study

(Schalow & Kunzek, 2004) observed the same phenomena where suspensions with rough particles showed better rheological properties compared to suspensions with smooth particles.

As discussed before, the improvement after HPH was suggested to happen due to the breakdown of particles, opening up of CWM structures and the aggregation of particles due to particle interactions. The microscopy visualization may not show a comprehensive description of the particle aggregation. The samples have to be diluted and mixed to clearly show the particle morphology which may have broken down some of the network formed from the aggregation. Nevertheless, some particle aggregations were still observed in the microscopy visualization of the suspension after HPH (Figure 4) which indicated the formation of a stronger network and thus lead to an increase of the G' after HPH.

The observation that the pulp AR suspensions have lower G' compared to the peel AR suspensions after HPH despite their rod-shaped particles, which should result in a bigger phase volume, suggests that other properties of the particles should be considered, such as their deformability, polydispersity, and especially the potential interactions between particles such as hydrophobic/hydrophilic interactions or repulsive/attractive forces due to charges for example from the pectin in the CWM (Genovese et al., 2007; Tsai & Zammouri, 1988). These properties are out of the scope of this study; however, they are interesting properties to be studied in the future.

3.2.2.2. Particle size distribution

Particle size is another microstructural characteristic that should be considered in the functionalization of the CWM. The particle size distribution of the suspension before HPH was

448 monomodal with a wide distribution and sometimes with a shoulder appearing on the larger
449 particle size region (Figure S-2 in Supplementary File). After HPH, the particle size distributions
450 became narrower and without shoulder and shifted to the smaller particle regions. In order to
451 compare the particle size between different citrus AR, the D_{50} of the particles in citrus AR
452 suspensions was shown in Figure 5. It was clear that HPH not only resulted in smaller particles
453 but also a more homogenous particle size distribution. The same observations were reported in
454 previous studies (Augusto et al., 2012; Bengtsson & Tornberg, 2011; Lopez-Sanchez et al., 2011;
455 Su et al., 2019; Zhou et al., 2017). The shear force on the particles that were pushed through the
456 small orifice in the homogenizer caused fragmentation resulting in a lower particle size. The
457 decrease in the particle size has been hypothesized to be essential in the functionalization of the
458 CWM into texturizing ingredients in this study. However, this decrease in the particle size was not
459 consistently observed in the homogenized CWM system. Some studies reported an increase in
460 the particle size after homogenization and they argued that the increase was caused by swelling
461 of the polysaccharides (Huang et al., 2020; Ulbrich & Flöter, 2014; Van Audenhove et al., 2021;
462 Willemsen et al., 2017).
463
464 Moreover, the rheological properties were clearly different among the citrus ARs in this study
465 although the D_{50} of the particles in the suspensions after HPH were not distinctive between the
466 different citrus ARs. Because of their complexity, even for very comparable matrices, the PSD of
467 a CWM dispersion system cannot be an indicator of the expected texturizing potential. The
468 interactions between the CWM particles, both intra- and inter-particle, probably largely determines
469 the rheological properties of the suspension. However, the elucidation of this interaction in a
470 complex CWM matrix is far more challenging and not straightforward.
471
472 *3.2.2.3. Monosaccharide content and pectin's DM*

The results from GalA and neutral sugar content analysis of the different citrus ARs are shown in Table 2. GalA is the main backbone monosaccharide of the pectin in the AR. The citrus ARs contained about 14-17 g GalA per 100 gram dry matter of the residue. This corresponds to about 13-23% of GalA content in the AIR that was retained in the citrus ARs (Table 1) which indicates that there was a substantial amount of unextracted pectin. The GalA content in the ARs from different species and fruit parts was not significantly different. Correlations were not detected between the GalA content of the citrus AR and the rheological properties of the suspensions. Thus, in this study, the pectin content of the ARs, as indicated by the GalA content, did not prompt the different rheological properties shown by suspensions from different raw materials.

On the other hand, the structural properties of the pectin may have an influence on the rheological properties of the suspension, especially before HPH. The structural properties of the residual pectin can be described by the Rha, Ara and Gal content of the ARs. Rha is one of the main backbone monosaccharides of the RG-I domain of the residual pectin. The peel ARs had significantly ($p \leq 0.001$) higher Rha, consequently more RG-I contribution in the residual pectin, compared to pulp residues. There were also significant differences ($p \leq 0.001$) in the Rha content among the citrus species, where orange residues showed the highest RG-I contribution in their residual pectin while grapefruit showed the least. Previous study on different citrus peel fibres (without pectin depletion) also showed that Rha content was highest for orange fibre compared to other citrus (Kaya et al., 2014). Ara and Gal content of the ARs can be linked to the side-chains of pectin, although in the current study, the value of Gal content cannot be fully attributed to the pectin side-chains since parts of the Gal content may be contributed by the side-chains of xyloglucan (Harris & Smith, 2006). Nevertheless, as the Ara and Gal content became higher (such as in orange ARs compared to lemon and grapefruit and in pulp ARs compared to peel ARs), the

G' of the AR suspension before HPH decreased. The same negative correlation ($p \leq 0.001$, $r = 0.786$) was observed between the Rha content of AR with the suspension G' value before homogenization. Previous studies have postulated that pectin interacts with cellulose through the RG-I region (Broxterman & Schols, 2018; Zykwinska et al., 2007) and through the side-chains or arabinan and galactan (Lin et al., 2016). Some of the pectin-cellulose interactions may have been broken down during the acid extraction process, but the remaining pectin was relatively more strongly bound. The interaction between the remaining pectin and the cellulose may cause the cell wall particles to be more resistant to opening up which is needed in order to create a suspension with good rheological properties as previously discussed. However, the pectin-cellulose interaction has proven to be weak (Lin et al., 2016), therefore HPH may have broken down the interaction, changed the characteristics of the particles, allowed the cell wall network to open up and eventually improved the G'. Consequently, the structure of the pectin as indicated by the Rha, Ara and Gal did not show correlation with the G' after HPH.

The pectin fraction left in the residues was characterized for its DM, and the results (Figure 6) showed that the pectin in the citrus ARs are considered high-DM pectin (DM value higher than 50%) (Harris & Smith, 2006). The pectin in the AR from grapefruit and lemon, both from the peel and pulp, have similar DM at approximately 70%. However, the pectin in the orange AR had lower DM than the others (57% and 64% in the peel and the pulp AR, respectively). Similar values and trends were reported in previous studies with orange pectin and orange fibre, where the DM ranged from 58% to 68% and the peel fibre showed a lower pectin DM compared to the pulp fibre (Lundberg et al., 2014; Schalow & Kunzek, 2004). The DM is an important structural characteristic of pectin as it affect the charge and the gelling mechanism of the pectin (Yoo et al., 2006) and it may also influence the way pectin interact with other polymers in the CWM. A previous study reported that the binding ability of higher DM pectin to cellulose in an *in vitro* system was slightly

lower than the low DM pectin, although they suggested that the DM is not a dominant factor affecting the interactions (Lin et al., 2016). In this study, the DM of the residual pectin were positively correlated to the G' of the suspension before HPH ($p \leq 0.001$, $r = 0.731$). ARs containing pectin with lower DM, such as orange peel, showed a lower G' of the suspension before HPH. However, after HPH, the correlation became weaker ($p \leq 0.05$, $r = 0.405$). This supported the hypothesis that the structural characteristics of the pectin may determine the rheological properties before HPH, however the effect of HPH is more dominant in determining the rheological properties of the suspension after HPH.

The most common and abundantly found hemicellulose in dicotyledon plant, including citrus fruits, is xyloglucan which is a branched polymer with β-D-glucan as the backbone and side chains consisting of xylosyl residues (Harris & Smith, 2006). Thus, Xyl can be a good indicator for the xyloglucan content in the residue. Citrus ARs contained 5.8 – 7.2 g Xyl / 100 g residue, the grapefruit peel AR contained the highest Xyl and the orange peel AR contained the lowest Xyl. Previous study reported the same trend in the Xyl content of different citrus peel fibres without pectin depletion (Kaya et al., 2014). Peel ARs generally have significantly ($p \leq 0.05$) higher Xyl content than pulp ARs. On the other hand, Man content can indicate the presence of another group of hemicellulose, mannan, that occurs in a lesser amount compared to xyloglucan in the citrus residue. There was 2.3 – 3.5 g of Man in 100 g of citrus residue and there was no significant difference in the Man content between peel and pulp residue. There were also no significant differences in the Man content between lemon and orange, while values for grapefruit residue were significantly lower than all others. The Xyl and Man content of the AR did not affect the rheological properties of the AR suspensions (no correlations).

547 Glu content (Table 2) obtained after matrix hydrolysis / Glu (mat) can be attributed to the non-
548 cellulosic polysaccharides, mainly from the hemicellulose (backbone of xyloglucan). Significant
549 differences in the Glu (mat) content between ARs from different citrus species were observed
550 ($p \leq 0.001$) where orange ARs showed the highest values while grapefruit AR showed the lowest.
551 A negative correlation ($p \leq 0.001$, $r = -0.833$) was observed between Glu (mat) content of the ARs
552 and the associated G' values of the suspensions before homogenization. In the cell wall matrix,
553 hemicellulose may act as a link between the cellulose microfibrils (Cosgrove, 1997). Prior to HPH,
554 the bounds may still have a strong influence on the matrix and they prevent the cell wall particles
555 to open up and create the gel-like network with high G'. However, no correlation was detected
556 between Glu (mat) content and the G' of the suspension after HPH. The Glu (mat) content may
557 also have affected the structural properties of the polysaccharides in the CWM in which the effect
558 disappeared after HPH.
559
560 The cellulose content in the AR was obtained from the difference between the glucose value from
561 Saeman hydrolysis and matrix hydrolysis, which was considered to be the glucose that built the
562 cellulose. The Glu content after Saeman hydrolysis was the most abundant sugar present in the
563 citrus AR, ranging from 48 to 60 g / 100 g residue (Table 2), which indicated that cellulose was
564 the most abundant polysaccharide in the residue. Grapefruit AR had significantly ($p \leq 0.001$) higher
565 cellulose content compared to other citrus species (50-57 g / 100 g residue compared to 41-48 g
566 / 100 g residue). The cellulose contents of the fruit peel and fruit pulp ARs from all the citrus
567 species were not significantly different. Suspensions from grapefruit and lemon ARs with higher
568 cellulose content than orange AR had higher G' both before and after HPH. Previous studies
569 (Ulbrich & Flöter, 2014) have shown that cellulose porosity increased after HPH which lead to
570 increased water retention capacity and swelling of the cellulose microfibril. Consequently a better
571 rheological properties were observed (Ulbrich & Flöter, 2014).

572

573 *3.2.2.4. Protein content*

574

575 Protein (in total of 3-8 g/100 g d.m.) was present in the different citrus ARs (Figure 7). The peel
576 ARs have significantly lower protein content than the pulp, meanwhile orange AR had the highest
577 protein content compared to the ARs from other citrus species. The protein in the AR is expected
578 to consist of different classes of cell-wall protein such as extensins, arabinogalactan protein,
579 proline-rich protein, and others. They are hydroxyproline-rich proteins and each of them have their
580 own function, structure and intermolecular interaction with other component of the cell wall
581 (Showalter, 1993; Sommer-Knudsen et al., 1998). The values of the protein content in the citrus
582 ARs was slightly smaller than values found in similar citrus materials in other studies (Chau &
583 Huang, 2003; Marín et al., 2007; Tripodo et al., 2004) in which the crude protein in various citrus
584 by-products were found to be between 7-12% d.m. The lower value in the AR in this study may
585 be due to the solubilization and/or degradation of the protein during the acid extraction process
586 with the heat and low pH.

587

588 The protein content of the citrus ARs and the G' of the suspension after HPH were significantly
589 correlated ($p<0.01$, $r = -0.524$). It can be hypothesized that the existence of protein, especially the
590 structural protein in the CWM, can inhibit the functionalization of the HPH. In this study, the peel
591 ARs, which have significantly lower protein content, have higher G' compared to the pulp ARs.
592 Orange ARs also have significantly higher protein content than the other citrus species and
593 consequently have a lower G'. A previous study supported the hypothesis, showing that both
594 heated pumpkin pomace (therefore denaturation of protein occurred) and deproteinated pumpkin
595 pomace had higher G' values compared to the untreated material (Atencio et al., 2021).

596

Structural proteins in the cell wall provide binding sites with other polysaccharides. For example, extensin, a structural protein found in cell wall, has been found to interact with acidic pectin, resulting in protein-polysaccharide crosslinks (Showalter, 1993; Sommer-Knudsen et al., 1998). These crosslinks may act as barrier in the unfolding and breaking down of the particles, a mechanism proposed for the improvement of the rheological properties after HPH of CWM suspensions discussed above.

4. Conclusions

This study demonstrated that the citrus ARs after pectin extraction are highly potential sources to be functionalized into texturizing ingredients using HPH. All citrus ARs, regardless of the species or the fruit part, had an improved G' after HPH. However, peel AR from lemon or grapefruit appeared to be a preferable source of CWM to be functionalized as they had higher G' compared to both their pulp counterpart and orange ARs. Lower protein content in the CWM materials, as in the peel AR from lemon and grapefruit, may contribute to a higher G' of the AR suspensions after HPH. The different citrus ARs also had different structural characteristics of the polymers as elucidated by the neutral sugar content and pectin DM analysis. They also had different microstructural characteristics as shown by microscopy visualization and particle size distribution. These characteristics may influence the rheological properties of the AR suspensions before HPH; however, they did not correlate to the rheological properties after HPH. The structural and microstructural properties of the CWM were changed due to particle fragmentation and aggregation during HPH which improved the rheological properties of the AR suspensions. Pectin extraction from the CWM prior to the functionalization is favourable to the improvement of the rheological properties since the removal of pectin leads to a more open structure which can encourage the fragmentation and aggregation / network formation of the particles. The intra- and

622 inter-particle interactions after HPH should be elucidated further to better understand the potential
623 of the CWM as texturizing ingredients.
624
625 **Acknowledgement**
626 Novita Ika Putri is a PhD fellow funded by collaboration with Cargill R&D Centre Europe. Jelle
627 Van Audenhove is funded by the Research Foundation Flanders (FWO) (grant number
628 1134619N).
629
630 **References**
631
632 Ahmed, E. R. A., & Labavitch, J. M. (1977). Method for accurate determination of cell wall.
633 *Journal of Food Biochemistry*, *1*(4), 361–365.
634 Atencio, S., Bernaerts, T., Liu, D., Reineke, K., Hendrickx, M., & Van Loey, A. (2021). Impact of
635 processing on the functionalization of pumpkin pomace as a food texturizing ingredient.
636 *Innovative Food Science and Emerging Technologies*, *69*(March), 102669.
637 https://doi.org/10.1016/j.ifset.2021.102669
638 Augusto, P. E. D., Ibarz, A., & Cristianini, M. (2012). Effect of high pressure homogenization
639 (HPH) on the rheological properties of tomato juice: Time-dependent and steady-state
640 shear. *Journal of Food Engineering*, *111*(4), 570–579.
641 https://doi.org/10.1016/j.jfoodeng.2012.03.015
642 Barnes, H. A. (2000). A Handbook of Elementary Rheology. In *Polymer Composites* (Vol. 6,
643 Issue 4).
644 Bengtsson, H., & Tornberg, E. (2011). Physicochemical characterization of fruit and vegetable
645 fiber suspensions. I: Effect of homogenization. *Journal of Texture Studies*, *42*(4), 268–280.
646 https://doi.org/10.1111/j.1745-4603.2010.00275.x

Blumenkrantz, N., & Asboe-Hansen, G. (1973). New Method for Quantitative Determination of Uronic Acids. *Analytical Biochemistry*, *54*, 484–489.

Broxterman, S. E., & Schols, H. A. (2018). Interactions between pectin and cellulose in primary plant cell walls. *Carbohydrate Polymers*, *192*(February), 263–272. https://doi.org/10.1016/j.carbpol.2018.03.070

Caggia, C., Palmeri, R., Russo, N., Timpone, R., Randazzo, C. L., Todaro, A., & Barbagallo, S. (2020). Employ of Citrus By-product as Fat Replacer Ingredient for Bakery Confectionery Products. *Frontiers in Nutrition*, *7*(April), 1–9. https://doi.org/10.3389/fnut.2020.00046

Chau, C. F., & Huang, Y. L. (2003). Comparison of the chemical composition and physicochemical properties of different fibers prepared from the peel of citrus sinensis L. Cv. Liucheng. *Journal of Agricultural and Food Chemistry*, *51*(9), 2615–2618. https://doi.org/10.1021/jf025919b

Cosgrove, D. J. (1997). Assembly and Enlargement of the Primary Cell Wall in Plants. *Annual Review of Cell and Developmental Biology*, *13*(1), 171–201. https://doi.org/10.1146/annurev.cellbio.13.1.171

FAO. (2021). Citrus fruit. In *Citrus Fruit Statistical Compendium 2020*. https://doi.org/10.5860/choice.36-2167

Fernandez-Gines, J. ., Fernandez-Lopez, J., Sayas-Barbera, E., Sendra, E., & Perez-Alvarez, J. . (2003). Effect of Storage Conditions on Quality Characteristics of Bologna Sausages Made with Citrus Fiber. *Journal of Food Science*, *68*(2), 710–715.

Genovese, D. B., Lozano, J. E., & Rao, M. A. (2007). The rheology of colloidal and noncolloidal food dispersions. *Journal of Food Science*, *72*(2). https://doi.org/10.1111/j.1750-3841.2006.00253.x

Harris, P. J., & Smith, B. G. (2006). Plant cell walls and cell-wall polysaccharides: Structures, properties and uses in food products. *International Journal of Food Science and*

672 *Technology*, *41*(SUPPL. 2), 129–143. https://doi.org/10.1111/j.1365-2621.2006.01470.x
673 Huang, X., Liu, Q., Yang, Y., & He, W. Q. (2020). Effect of high pressure homogenization on
674 sugar beet pulp: Rheological and microstructural properties. *Lwt*, *125*(January).
675 https://doi.org/10.1016/j.lwt.2020.109245
676 Hyun, K., Kim, S. H., Ahn, K. H., & Lee, S. J. (2002). Large amplitude oscillatory shear as a way
677 to classify the complex fluids. *Journal of Non-Newtonian Fluid Mechanics*, *107*(1–3), 51–
678 65. https://doi.org/10.1016/S0377-0257(02)00141-6
679 Kaya, M., Sousa, A. G., Crépeau, M. J., Sørensen, S. O., & Ralet, M. C. (2014).
680 Characterization of citrus pectin samples extracted under different conditions: Influence of
681 acid type and pH of extraction. *Annals of Botany*, *114*(6), 1319–1326.
682 https://doi.org/10.1093/aob/mcu150
683 Korus, J., Juszczak, L., Witczak, M., & Ziobro, R. (2020). Effect of citrus fiber on the rheological
684 properties of dough and quality of the gluten-free bread. *Applied Sciences (Switzerland)*,
685 *10*(19). https://doi.org/10.3390/APP10196633
686 Kyomugasho, C., Christiaens, S., Shpigelman, A., Van Loey, A. M., & Hendrickx, M. E. (2015).
687 FT-IR spectroscopy, a reliable method for routine analysis of the degree of
688 methylesterification of pectin in different fruit- and vegetable-based matrices. *Food*
689 *Chemistry*, *176*, 82–90. https://doi.org/10.1016/j.foodchem.2014.12.033
690 Lin, D., Lopez-Sanchez, P., & Gidley, M. J. (2016). Interactions of pectins with cellulose during
691 its synthesis in the absence of calcium. *Food Hydrocolloids*, *52*, 57–68.
692 https://doi.org/10.1016/j.foodhyd.2015.06.004
693 Lopez-Sanchez, P., Chapara, V., Schumm, S., & Farr, R. (2012). Shear Elastic Deformation and
694 Particle Packing in Plant Cell Dispersions. *Food Biophysics*, *7*(1), 1–14.
695 https://doi.org/10.1007/s11483-011-9237-9
696 Lopez-Sanchez, P., Nijsse, J., Blonk, H. C. G., Bialek, L., Schumm, S., & Langton, M. (2011).

Effect of mechanical and thermal treatments on the microstructure and rheological properties of carrot, broccoli and tomato dispersions. *Journal of the Science of Food and Agriculture*, *91*(2), 207–217. https://doi.org/10.1002/jsfa.4168

Lundberg, B., Pan, X., White, A., Chau, H., & Hotchkiss, A. (2014). Rheology and composition of citrus fiber. *Journal of Food Engineering*, *125*(1), 97–104. https://doi.org/10.1016/j.jfoodeng.2013.10.021

Marín, F. R., Soler-Rivas, C., Benavente-García, O., Castillo, J., & Pérez-Alvarez, J. A. (2007). By-products from different citrus processes as a source of customized functional fibres. *Food Chemistry*, *100*(2), 736–741. https://doi.org/10.1016/j.foodchem.2005.04.040

McFeeters, R. F., & Armstrong, S. A. (1984). Measurement of pectin methylation in plant cell walls. *Analytical Biochemistry*, *139*(1), 212–217. https://doi.org/10.1016/0003-2697(84)90407-X

Rao, M. A. (2014). *Rheology of Fluid, Semisolid and Solid Foods.pdf* (G. V Barbosa-Canovas (ed.); Third Edit).

Satari, B., & Karimi, K. (2018). Citrus processing wastes: Environmental impacts, recent advances, and future perspectives in total valorization. *Resources, Conservation and Recycling*, *129*(September 2017), 153–167. https://doi.org/10.1016/j.resconrec.2017.10.032

Schalow, S., & Kunzek, H. (2004). The influence of predrying treatment and of suspension solution conditions on the rehydration of apple cell wall materials. *European Food Research and Technology*, *219*(4), 329–340. https://doi.org/10.1007/s00217-004-0949-7

Sendra, E., Kuri, V., Fernández-López, J., Sayas-Barberá, E., Navarro, C., & Pérez-Alvarez, J. A. (2010). Viscoelastic properties of orange fiber enriched yogurt as a function of fiber dose, size and thermal treatment. *LWT - Food Science and Technology*, *43*(4), 708–714. https://doi.org/10.1016/j.lwt.2009.12.005

Showalter, A. M. (1993). Structure and function of plant cell wall proteins. *The Plant Cell*, *5*, 9–23. https://doi.org/10.1016/B978-0-08-092615-5.50014-X

Sommer-Knudsen, J., Bacic, A., & Clarke, A. E. (1998). Hydroxyproline-rich plant glycoproteins. *Phytochemistry*, *47*(4), 483–497. https://doi.org/10.1016/S0031-9422(97)00724-3

Song, J., Pan, T., Wu, J., & Ren, F. (2016). The improvement effect and mechanism of citrus fiber on the water-binding ability of low-fat frankfurters. *Journal of Food Science and Technology*, *53*(12), 4197–4204. https://doi.org/10.1007/s13197-016-2407-5

Su, D., Zhu, X., Wang, Y., Li, D., & Wang, L. (2019). Effects of high-pressure homogenization on physical and thermal properties of citrus fiber. *Lwt*, *116*(August). https://doi.org/10.1016/j.lwt.2019.108573

Su, D., Zhu, X., Wang, Y., Li, D., & Wang, L. (2020). Effect of high-pressure homogenization on rheological properties of citrus fiber. *Lwt*, *127*(April), 109366. https://doi.org/10.1016/j.lwt.2020.109366

Tripodo, M. M., Lanuzza, F., Micali, G., Coppolino, R., & Nucita, F. (2004). Citrus waste recovery : a new environmentally friendly procedure to obtain animal feed. *Bioresource Technology*, *91*, 111–115. https://doi.org/10.1016/S0960-8524(03)00183-4

Tsai, S. C., & Zammouri, K. (1988). Role of Interparticular Van der Waals Force in Rheology of Concentrated Suspensions. *Journal of Rheology*, *32*(7), 737–750. https://doi.org/10.1122/1.549988

Ulbrich, M., & Flöter, E. (2014). Impact of high pressure homogenization modification of a cellulose based fiber product on water binding properties. *Food Hydrocolloids*, *41*, 281–289. https://doi.org/10.1016/j.foodhyd.2014.04.020

Van Audenhove, J., Bernaerts, T., De Smet, V., Delbaere, S., Van Loey, A. M., & Hendrickx, M. E. (2021). The structure and composition of extracted pectin and residual cell wall material from processing tomato: The role of a stepwise approach versus high-pressure

homogenization-facilitated acid extraction. *Foods*, *10*(5). https://doi.org/10.3390/foods10051064

Van Audenhove, J., Bernaerts, T., Putri, N. I., Okello, E. O., Van Rooy, L., Van Loey, A. M., & Hendrickx, M. E. (2021). Microstructural and Texturizing Properties of Partially Pectin-Depleted Cell Wall Material : The Role of Botanical Origin and High-Pressure Homogenization. *Foods*, *10*(2644). https://doi.org/https://doi.org/10.3390/foods10112644

Verrijssen, T. A. J., Vanierschot, M., Ongena, S. I. M., Cardinaels, R., Van den Bulck, E., Van Loey, A. M., Hendrickx, M. E., & Van Buggenhout, S. (2014). Role of mechanical forces in the stomach phase on the in vitro bioaccessibility of β-carotene. *Food Research International*, *55*, 271–280. https://doi.org/10.1016/j.foodres.2013.11.017

Willemsen, K. L. D. D., Panozzo, A., Moelants, K., Cardinaels, R., Wallecan, J., Moldenaers, P., & Hendrickx, M. (2018). Effect of pH and salts on microstructure and viscoelastic properties of lemon peel acid insoluble fiber suspensions upon high pressure homogenization. *Food Hydrocolloids*, *82*, 144–154. https://doi.org/10.1016/j.foodhyd.2018.04.005

Willemsen, K. L. D. D., Panozzo, A., Moelants, K., Debon, S. J. J., Desmet, C., Cardinaels, R., Moldenaers, P., Wallecan, J., & Hendrickx, M. E. G. (2017). Physico-chemical and viscoelastic properties of high pressure homogenized lemon peel fiber fraction suspensions obtained after sequential pectin extraction. *Food Hydrocolloids*, *72*, 358–371. https://doi.org/10.1016/j.foodhyd.2017.06.020

Yeats, T., Vellosillo, T., Sorek, N., Ibáñez, A., & Bauer, S. (2016). Rapid Determination of Cellulose, Neutral Sugars, and Uronic Acids from Plant Cell Walls by One-step Two-step Hydrolysis and HPAEC-PAD. *Bio-Protocol*, *6*(20), 1–14. https://doi.org/10.21769/bioprotoc.1978

Yoo, S. H., Fishman, M. L., Hotchkiss, A. T., & Hyeon, G. L. (2006). Viscometric behavior of high-methoxy and low-methoxy pectin solutions. *Food Hydrocolloids*, *20*(1), 62–67.

https://doi.org/10.1016/j.foodhyd.2005.03.003

Zema, D. A., Calabrò, P. S., Folino, A., Tamburino, V., Zappia, G., & Zimbone, S. M. (2018). Valorisation of citrus processing waste: A review. *Waste Management*, *80*, 252–273. https://doi.org/10.1016/j.wasman.2018.09.024

Zhou, L., Guan, Y., Bi, J., Liu, X., Yi, J., Chen, Q., Wu, X., & Zhou, M. (2017). Change of the rheological properties of mango juice by high pressure homogenization. *Lwt*, *82*, 121–130. https://doi.org/10.1016/j.lwt.2017.04.038

Zykwinska, A., Thibault, J. F., & Ralet, M. C. (2007). Organization of pectic arabinan and galactan side chains in association with cellulose microfibrils in primary cell walls and related models envisaged. *Journal of Experimental Botany*, *58*(7), 1795–1802. https://doi.org/10.1093/jxb/erm037

Table 1. GalA content of the AIR and AR of different raw materials and the calculated percentage of unextracted GalA *average from 2 times extraction

Sample	GalA in AIR (g/60g AIR)	Yield of AR (g dry AR/60 g AIR)*	GalA in AR from 60 g of AIR (g)*	%GalA unextracted*
I-L-PE	22.3 ± 3.2	22.2	3.55	15.9
I-L-PU	22.0 ± 1.5	26.4	4.98	22.5
G-PE	24.5 ± 0.7	28.8	4.95	20.2
G-PU	25.8 ± 0.4	21.9	3.52	13.6
O-PE	19.1 ± 0.6	29.4	4.48	23.5
O-PU	21.8 ± 0.6	20.9	3.06	14.0
L-PE	20.3 ± 0.9	25.6	4.17	20.5
L-PU	23.1 ± 0.8	22.1	3.68	15.9

Table 2. Monosaccharides content (g/100 g d.m residue) and cellulose content (g/100 g d.m residue) estimation of the different citrus ARs. Values expressed were mean ± standard deviation (n=4).

Sample	Fuc	Rha	Ara	Gal	Glu (mat)	Glu (sae)	Xyl	Man	GalA	Cellulose content
G-PE	0.40 ± 0.25	1.07 ± 0.69	1.70 ± 0.42	4.00 ± 0.15	2.57 ± 0.44	59.90 ± 2.14	7.21 ± 0.39	2.50 ± 0.41	17.16 ± 1.04	57.33 ± 2.27
G-PU	0.16 ± 0.09	0.61 ± 0.24	1.87 ± 0.27	4.37 ± 0.40	3.89 ± 0.92	54.68 ± 1.94	6.25 ± 0.63	2.34 ± 0.69	16.00 ± 1.02	50.79 ± 1.79
O-PE	0.16 ± 0.08	3.38 ± 0.28	2.12 ± 0.16	5.34 ± 0.16	6.96 ± 0.40	48.14 ± 3.04	5.74 ± 0.28	2.88 ± 0.07	15.28 ± 0.71	41.18 ± 3.25
O-PU	0.14 ± 0.06	1.96 ± 0.17	2.26 ± 0.20	6.35 ± 0.54	4.57 ± 0.27	49.45 ± 4.43	5.84 ± 0.41	3.18 ± 0.25	14.67 ± 1.10	44.89 ± 4.49
L-PE	0.62 ± 0.03	2.13 ± 0.02	2.01 ± 0.12	5.93 ± 0.13	5.15 ± 0.24	52.71 ± 1.37	6.86 ± 0.18	3.55 ± 0.06	16.29 ± 1.34	47.56 ± 1.43
L-PU	0.51 ± 0.05	0.96 ± 0.05	2.46 ± 0.07	5.83 ± 0.04	3.67 ± 0.30	50.17 ± 2.00	5.82 ± 0.30	3.11 ± 0.16	16.64 ± 1.36	46.50 ± 1.96

Table 3. F values and the significance level from Two-Way ANOVA for the effect of citrus species and fruit part on the parameters (*p≤0.05 ; **p≤0.01 ; ***p≤0.001 ; ^{ns} : non-significant)

Parameter	Citrus Species	Fruit Part	Citrus Species x Fruit Part
G' (0 MPa)	93.29***	3.06^{ns}	31.54***
G' (20 MPa)	150.30***	50.69***	2.41^{ns}
D50 (0 MPa)	1.13^{ns}	68.54***	6.96**
D50 (20 MPa)	37.97***	0.06^{ns}	10.66***
Fuc	28.45***	5.12*	1.80^{ns}
Rha	84.02***	60.52***	6.93**
Ara	17.22***	15.49***	2.37^{ns}
Gal	105.58***	27.03***	3.31^{ns}
Glu (mat)	69.65***	14.46*	36.45***
Glu (sae)	20.40***	0.21^{ns}	0.23^{ns}
Xyl	4.08*	6.93*	2.62^{ns}
Man	24.64***	0.03^{ns}	1.63^{ns}
GalA	0.79^{ns}	0.29^{ns}	1.51^{ns}
Cellulose content	33.97***	1.89^{ns}	3.82*
DM	41.64***	30.53***	1.27^{ns}
Protein content	76.28***	2914.08***	11.52***

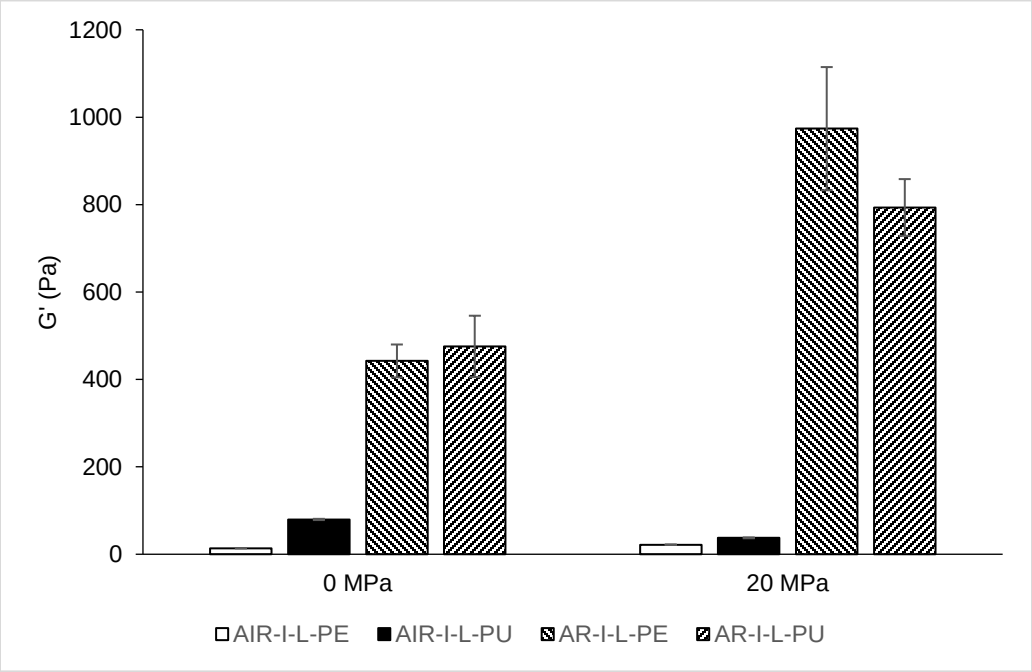

Figure 1. Storage modulus of suspensions from AIR and AR at frequency 6.28 rad/s before HPH (0 MPa) and after HPH (20 MPa). Value expressed were mean; vertical bars represents standard deviation for each mean.

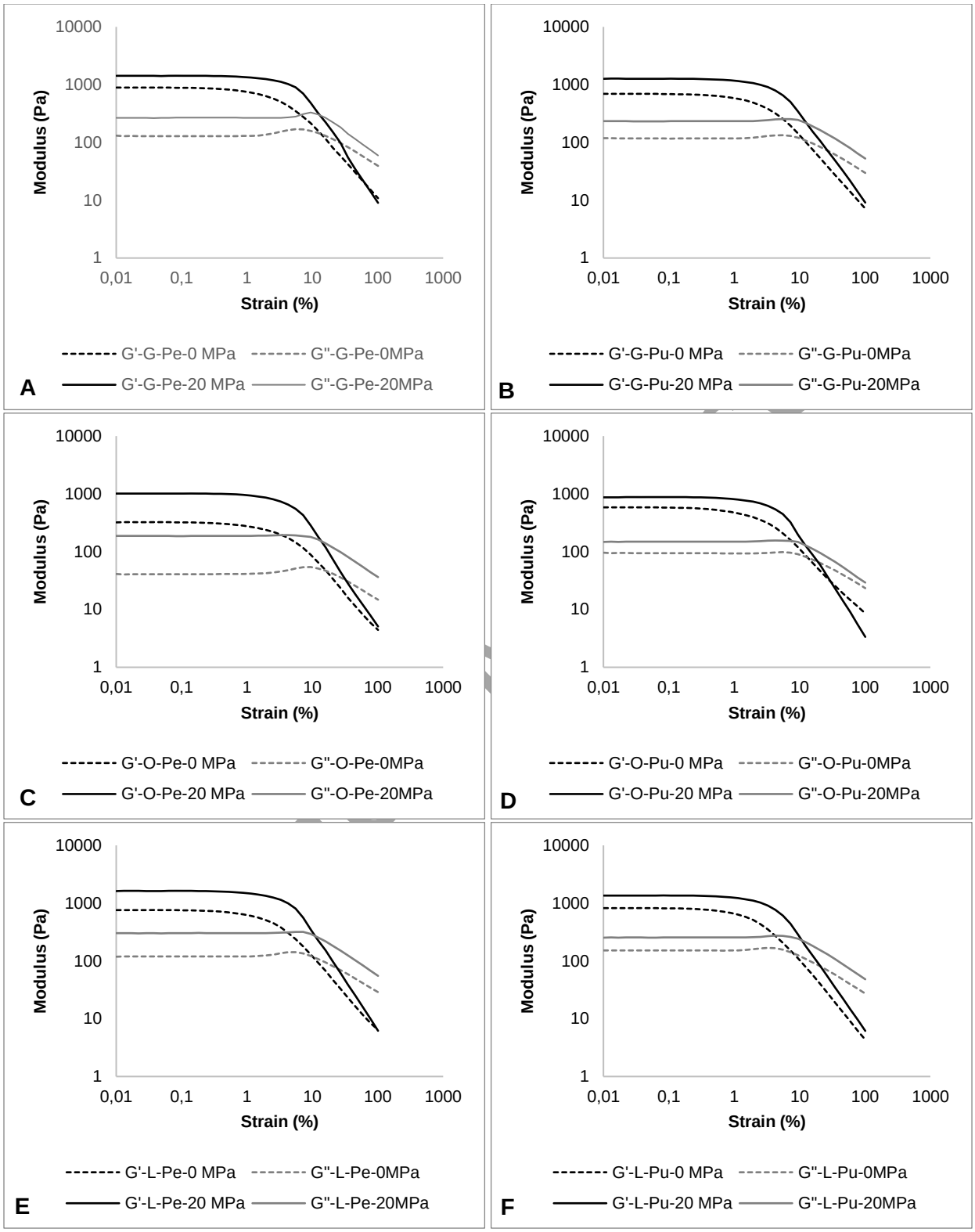

Figure 2. Storage (G') and loss modulus (G") as a function of strain of the suspensions before (0 MPa) and after HPH (20 MPa) from different citrus ARs : (A) Grapefruit peel (G-PE) (B) Grapefruit pulp (G-PU) (C) Orange peel (O-PE) (D) Orange pulp (O-PU) (E) Lemon peel (L-PE) (F) Lemon pulp (L-PU)

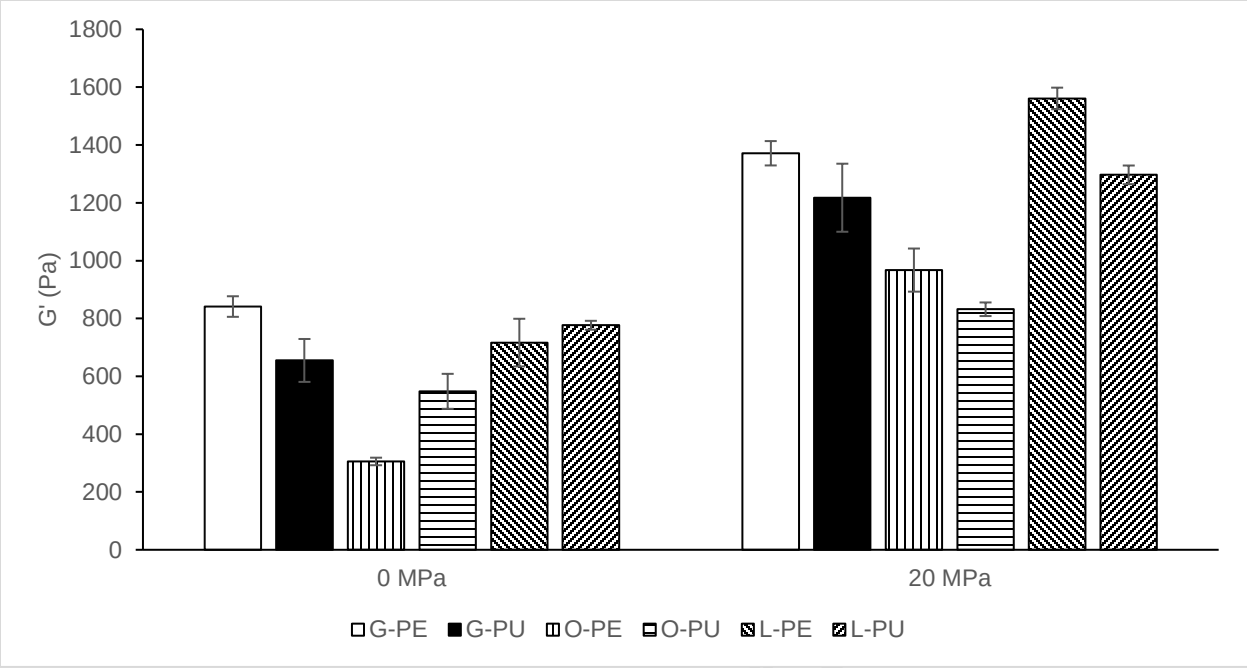

Figure 3. Storage modulus of suspensions from different citrus ARs at frequency 6.28 rad/s before HPH (0 MPa) and after HPH (20 MPa). Value expressed were mean (n=4); vertical bars represents standard deviation for each mean.

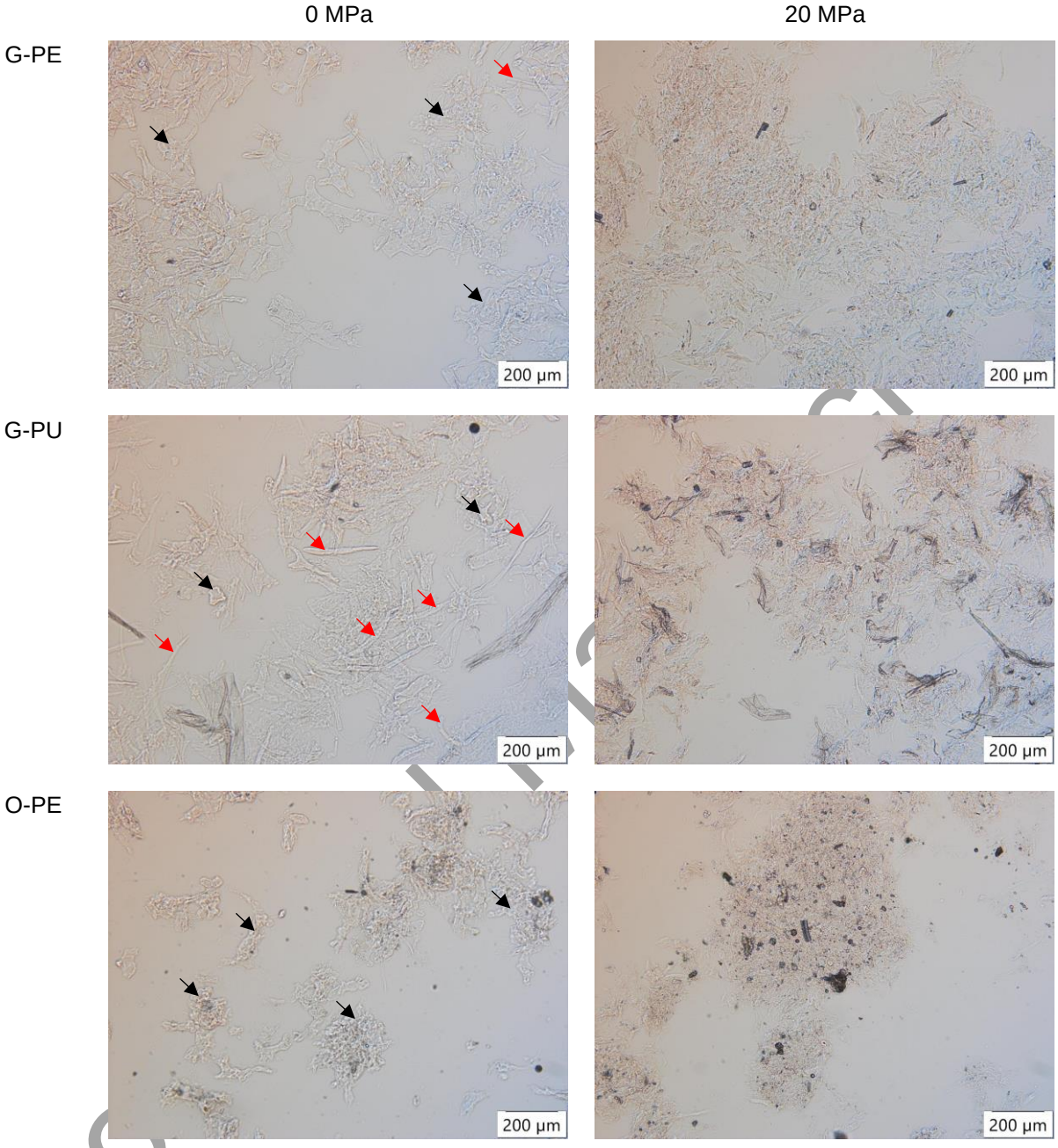

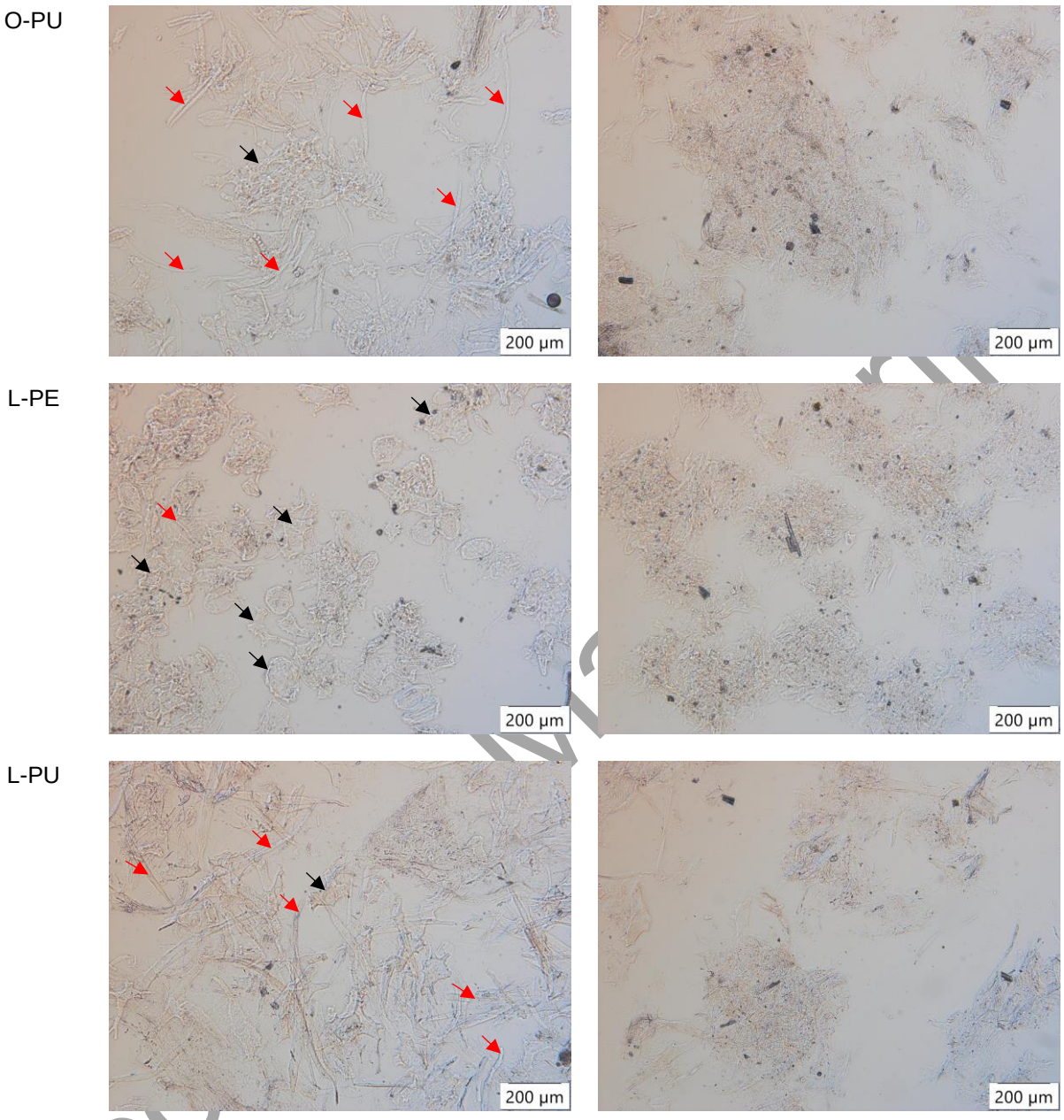

Figure 4. Microscopic visualization of the particles in the suspensions from different citrus ARs (at 0.6% w/w solid concentration) before HPH (0 MPa) and after HPH (20 MPa). Red arrow indicate fibrous (rod-like) particles and black arrows indicate irregularly shaped particles.

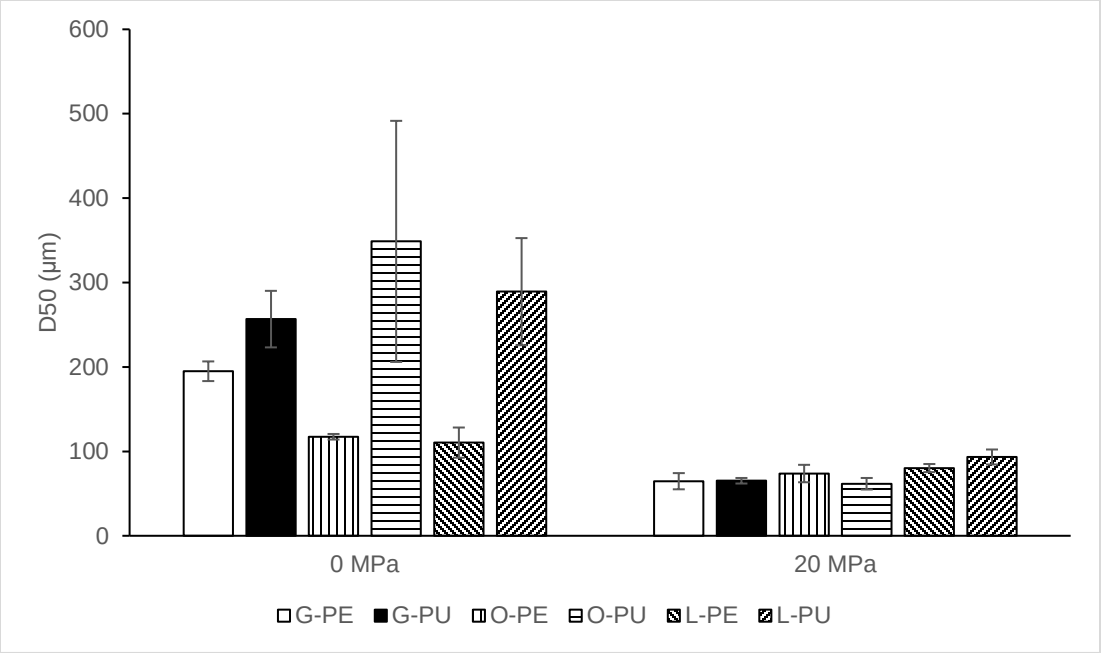

Figure 5. Median volumetric diameter (D50) of the particle in the suspensions from different citrus ARs before HPH (0 MPa) and after HPH (20 MPa). Value expressed were mean (n=8); vertical bars represents standard deviation for each mean.

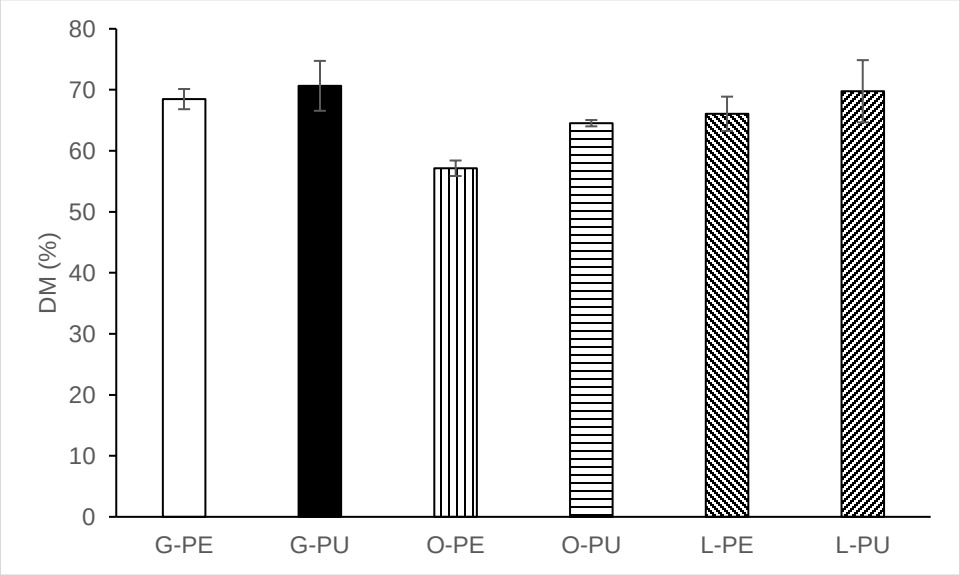

Figure 6. Degree of methyl-esterification of the residual pectin in the citrus ARs. Value expressed were mean (n=6); vertical bars represents standard deviation for each mean.

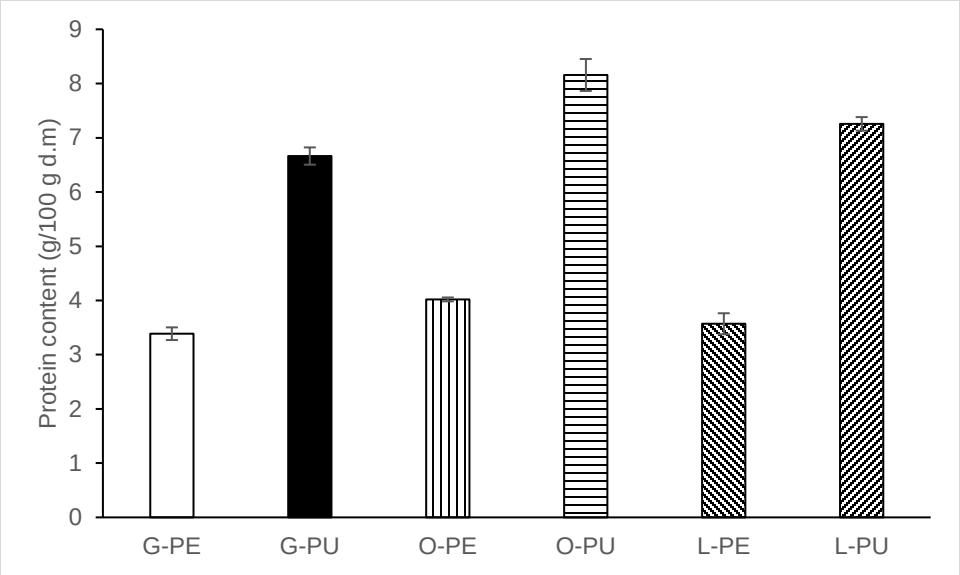

Figure 7. Protein content of the citrus ARs. Value expressed were mean (n=4); vertical bars represents standard deviation for each mean.